

Declining hydraulic performances and low carbon investments in tree rings predate Scots pine drought-induced mortality

Ana-Maria Hereş · Jesús Julio Camarero ·
Bernat C. López · Jordi Martínez-Vilalta

Received: 19 June 2014 / Accepted: 18 August 2014
© Springer-Verlag Berlin Heidelberg 2014

Abstract

Key message The retrospective analysis of wood anatomical features evidences how a long-term deterioration of hydraulic performance and carbon use portend drought-induced mortality in Scots pine.

Abstract Widespread episodes of drought-induced tree mortality are predicted to become more frequent as climate becomes warmer and drier. Nevertheless, growth trends and their links to changes in wood anatomy before tree dies are still poorly understood. Wood anatomical features provide valuable information that can be extracted to infer the mechanisms leading to tree death. In this study, we characterize drought-induced mortality affecting two Scots pine (*Pinus sylvestris*) sites (Prades and Arcalís) located in the North Eastern Iberian Peninsula. Co-occurring now-dead and living Scots pine trees were sampled and their wood anatomical features were measured and compared. We aimed to detect differences in anatomical features between living and dead trees, and to infer past physiological performances that might have determined their

subsequent death or survival. Now-dead trees showed lower tracheid and resin duct production, and smaller radial lumen diameters than co-occurring living trees. At the more xeric Prades site, these anatomical differences were larger and chronic, i.e. were observed over the three studied decades, whilst they were less pronounced at the other, more mesic Arcalís site, where tree mortality episodes were more recent. This indicates that dead trees' hydraulic conductivity was severely affected and that carbon investment in xylem formation and resin duct production was constrained prior to tree death. Our findings show that both hydraulic deterioration and low carbon allocation to xylem formation were associated to drought-induced mortality in Scots pine. Nevertheless, the temporal dynamics of these processes differed between populations as a function of site climatic conditions.

Keywords Scots pine · Mortality · Drought · Tree ring · Tracheid · Wood anatomy

Communicated by E. Liang.

Electronic supplementary material The online version of this article (doi:10.1007/s00468-014-1081-3) contains supplementary material, which is available to authorized users.

A.-M. Hereş · B. C. López · J. Martínez-Vilalta
CREAF, Cerdanyola del Vallès, 08193 Barcelona, Spain

A.-M. Hereş · B. C. López · J. Martínez-Vilalta
Universitat Autònoma de Barcelona, Cerdanyola del Vallès,
08193 Barcelona, Spain

J. J. Camarero (✉)
Instituto Pirenaico de Ecología (IPE-CSIC), Avda. Montañana
1005, 50059 Zaragoza, Spain
e-mail: jjcamarero@ipe.csic.es

Introduction

Episodes of drought-associated tree mortality have been reported in all major forest biomes (Allen et al. 2010), and are likely to become more frequent under a progressively warmer and drier climate (IPCC 2013). Consequently, understanding the mechanisms that underlie tree mortality has become a research priority in drought-prone areas. In Mediterranean regions like the Iberian Peninsula, water availability is the main limiting factor for tree growth (Cherubini et al. 2003; Martínez-Vilalta et al. 2008 and references therein). In these regions, temperature and evapotranspiration have increased during the last decades, in concert with the frequency and intensity of severe

droughts (Piñol et al. 1998; IPCC 2013). Thus, Mediterranean forests are considered to be especially vulnerable to this predicted increase of severe drought events (Giorgi and Lionello 2008). This is particularly the case for forests dominated by species reaching their southern (and dry) distribution limit in this region (e.g., Martínez-Vilalta et al. 2012; Matías and Jump 2012).

The mechanisms that underlie drought-induced tree mortality are still poorly understood and highly debated (McDowell et al. 2008, 2011; Sala et al. 2010; McDowell and Sevanto 2010; McDowell 2011; Sevanto et al. 2014). The efficiency and safety of the water transport through the xylem are critical for tree performance, especially under stressful climatic conditions such as those imposed by droughts (e.g., Choat et al. 2012). Trees growing in dry areas must maintain a functional water transport system by keeping the xylem water potentials above cavitation thresholds when facing drought events (Bréda et al. 2006; Brodribb and Cochard 2009). In the case of conifers, building tracheids with narrow lumens and thick walls might be advantageous under these circumstances, as the risk of cavitation and cell collapse generally decreases with smaller lumen diameter and thicker cell walls (Hacke et al. 2001; Cochard et al. 2004). Conduit lumen size is reduced when trees face water stress, because radial enlargement of tracheids is particularly sensitive to water deficit (Hsiao and Acevedo 1974; von Wilpert 1991). However, tracheids that have a reduced lumen diameter are less efficient for water transport, as the hydraulic conductivity increases with the fourth power of lumen diameter according to the Hagen–Poiseuille law (Tyree and Zimmerman 2002). Finally, prolonged water deficit can affect tracheid division and xylogenesis to such a degree that later on precipitations might not be able to compensate for past cumulative stress. As a consequence, narrow rings formed by low numbers of narrow tracheids are built, resulting into reduced water supply to the crown (Zweifel et al. 2006). The formation of narrow rings involves a low carbon investment in radial growth. Regardless of whether this low carbon investment under drought reflects low carbon availability, or simply the direct effect of lower water availability (Hsiao and Acevedo 1974; Sala et al. 2010), it has relevant implications for the tree's carbon economy and for the likelihood of carbon starvation (McDowell 2011).

Defence is another important component of the tree's response to drought stress particularly when biotic agents are involved (e.g., Gaylord et al. 2013). Resin ducts are a key component of tree defence against biotic agents (Paine et al. 1997; Rigling et al. 2003). Low resin duct production under drought might reflect reduced carbon availability to defence (McDowell et al. 2008; Sala et al. 2010) and increases the vulnerability of trees to biotic attack (Kane and Kolb 2010; Gaylord et al. 2013).

Wood anatomy studies on dead/dying vs. living trees are still scarce (but see Levanič et al. 2011), yet they can bring retrospective information about mortality processes, because xylem represents a reliable and long-term proxy of hydraulic performance. A retrospective analysis of the potential hydraulic performance of trees is feasible through wood anatomical analyses, which constitute a powerful tool for investigating tree responses to past stress conditions (Vaganov et al. 2006) at a higher temporal resolution than tree rings (Fritts 2001). The environmental conditions during wood formation determine xylem cells' features, leaving permanent imprints at the conduit level (Denne and Dodd 1981; Wimmer 2002; Fonti et al. 2010). The long-term theoretical hydraulic performance of a tree can be thus reconstructed through the analyses of anatomical features of transversal wood sections.

Several episodes of drought-induced mortality of Scots pine (*Pinus sylvestris* L.) have been reported in Europe over the last decades (Martínez-Vilalta and Piñol 2002; Bigler et al. 2006; Eilmann et al. 2006; Galiano et al. 2010; Camarero et al. 2012; Hereş et al. 2012; Vilà-Cabrera et al. 2013; Rigling et al. 2013). Scots pine is a boreal tree species, considered the most widely distributed conifer in the world (Nikolov and Helmisaari 1992). It reaches its south-western (and dry) distribution limit in the Iberian Peninsula (Barbéro et al. 1998), where about half of its range is represented by natural populations (Catalan Bachiller et al. 1991; Martín et al. 2010). Scots pine is a “drought-avoiding” species, with a relatively high vulnerability to xylem embolism (Cochard 1992) and a fast stomatal response to reduce evaporative water loss under drought conditions (Irvine et al. 1998; Poyatos et al. 2013). Consistent with its wide distribution, it shows high intra-specific variability in many traits, including wood anatomical ones (Martín et al. 2010).

In this study, we compare the wood anatomy of co-occurring now-dead and living Scots pine trees sampled at two climatically contrasted sites located in North Eastern Iberian Peninsula. The analyses are conducted at an annual resolution for a period of 34 years (1975–2008). Previous studies on the same individuals showed that tree mortality was associated with severe drought periods, and that now-dead individuals started to grow less than their surviving neighbours 15–40 years before death (Hereş et al. 2012). Our main objective here was to compare the stem xylem structure of now-dead trees and their surviving neighbours during the period previous to death. We retrospectively describe annual wood anatomical variability in terms of hydraulic conductivity and carbon investment in xylem structure and defence. More specifically, we aimed at establishing whether now-dead trees were more vulnerable to xylem embolism than living ones, or had an impaired hydraulic system due to the production of very narrow

tracheids or reduced their carbon investment in the xylem, which could reflect low carbon availability.

Materials and methods

Study sites

Two Scots pine sites located in the North Eastern Iberian Peninsula were selected: Prades (Prades Mountains, 41°19'N, 1°0'E) and Arcalís (Soriguera, Central Pyrenees, 42°22'N, 1°11'E). At these two sites, high mortality rates following particularly dry years have been observed starting in the 1990s (Martínez-Vilalta and Piñol 2002; Galiano et al. 2010; Poyatos et al. 2013). In addition, a direct association between tree mortality and severe drought periods characterized by low summer water availability has been reported leading to a long-term growth divergence between living and recently dead trees, particularly at the more xeric Prades site (Hereş et al. 2012). The climate in Prades is typically Mediterranean whilst in Arcalís it is characterized by cool-summer Mediterranean conditions (Köppen 1936). Mean annual temperature in Prades is around 11.2 °C, and the mean annual rainfall is 611 mm. In Arcalís, the mean annual temperature is lower (9.7 °C), and the mean annual rainfall is slightly higher (653 mm) than in Prades (Climatic Digital Atlas of Catalonia, period 1951–2006 in both cases) (Pons 1996; Ninyerola et al. 2000). A significant warming trend has been detected in both study sites over the last decades (Supplementary Fig. 1). The vegetation type at the two sites follows an altitudinal gradient, with Mediterranean species at low altitudes and Scots pine appearing above 800 m in Prades and between 600 and 1500 m in Arcalís. The soils in Prades are xerochrepts with a clay-loam texture (Hereter and Sánchez 1999), and in Arcalís they are calcareous with a clay-loam texture (Galiano et al. 2010). At both sites, soils have a low water retention capacity.

Field sampling

Scots pine trees used in this study were sampled in late autumn 2008 (Prades) and early spring 2009 (Arcalís) along constant altitude transects (1,000 m a.s.l for both sites) located on north facing slopes. Sampling consisted in coring co-occurring living and dead individuals at breast height (1.3 m), using increment borers, orthogonally to the slope. Here, we use 20 trees (10 per site: 5 living and 5 dead trees) that were visually cross-dated using pointer years in a previous study, from where basal area increment (BAI, cm²) and tree-ring width (mm) data were available (Hereş et al. 2012). Dead individuals used in this study died (last ring formed) between 2001 and 2008. Living and

dead trees did not differ significantly in terms of diameter at breast height (DBH) neither in Prades ($P = 0.793$, mean \pm SD = 32.0 \pm 5.1 cm) nor in Arcalís ($P = 0.533$, mean \pm SD = 33.0 \pm 5.0 cm). The age of the living and dead trees was also similar both in Prades ($P = 0.144$, mean \pm SD = 98 \pm 30 years) and Arcalís ($P = 0.411$, mean \pm SD = 69 \pm 9 years). Sampled trees were separated from each other or from other adult Scots pines, by a distance of at least 5 m. See Hereş et al. (2012) for additional sampling details.

Wood anatomy measurements

The segments of the cores that included the 1975–2008 period were separated into small blocks (about 1 cm long) that were further cut transversally with a sliding microtome (Leica SM 2010R; Leica Microsystems, Germany) to obtain thin wood sections (12–18 μ m thick). These sections were stained with a mixture of safranin (0.5 %) and astrablue (1 %) to get a better contrast between tracheid lumen and walls, dehydrated repeatedly in an alcohol concentration gradient (50–96 %) and mounted using a synthetic resin (Eukitt; Merck, Darmstadt, Germany) onto permanent glass microscope slides. Images of the thin wood sections were taken at magnifications of $\times 40$ using a camera (Leica DFC290; Leica Microsystems, Germany) attached to a transmitted light microscope (Olympus BH2; Olympus, Hamburg, Germany). When tree rings were too wide to fit in one image, several adjacent pictures were taken and then merged using Adobe Photoshop CS4 (Adobe Systems; San Jose, USA). The images were later on used to analyse a total of 646 annual rings using DACiA (Dendrochronological Analysis of Conifer Wood Anatomy), a new Matlab[®]-based (version 7.10 R2010a, MathWorks, Natick, MA) software developed specifically for this study (see next section on Software used to quantify wood anatomy, DACiA).

Tracheids were measured along 3–5 complete radial rows to obtain average values per measured ring since this number of rows provides a robust estimate of wood anatomical variability across the whole ring (Seo et al. 2014). We selected complete rows of well-developed tracheids, i.e. transversally fully expanded cells with complete walls, representing the structure of each measured ring. Measured variables, analysed at the whole ring level (RW) and separately for the earlywood (EW) and latewood (LW), included number of tracheids, radial lumen diameter (LD) and cell wall thickness (CWT). The visual identification of LW, based on the abrupt shifts in colour and tracheid size, was preferred over the delineation based on the Mork index (Denne 1988), which proved to largely overestimate LW in our samples. Radial dimensions were chosen because they vary along time, whilst the tangential dimensions are

effectively constant (Vysotskaya and Vaganov 1989). Using the measured anatomical features listed above, we calculated the theoretical tree-ring-based hydraulic conductivity (K_h) according to the Hagen–Poiseuille law (Tyree and Zimmerman 2002), the $(CWT/LD)^2$ ratio (Hacke et al. 2001), here used as a surrogate of the xylem vulnerability to embolism, and the tracheid carbon cost investments (C_{cost}). The $(CWT/LD)^2$ ratio is considered a reasonable anatomical proxy of xylem resistance to embolism, at least across species (Hacke et al. 2001). C_{cost} was estimated by multiplying the number of tracheids by CWT for each tree ring. To estimate the carbon allocation for defence (Kane and Kolb 2010), we counted the number of resin ducts produced per annual ring (RD), i.e. across the 5-mm window defined by the core size.

A selection of the measured wood anatomical features was used in further analyses, their subscript indicating if they refer to RW, EW or LW (Table 1). This selection was mainly based on the concept that EW has predominantly a water conductive function, whilst LW has mainly a mechanical one (Eilmann et al. 2006; Vaganov et al. 2006).

Software used to quantify wood anatomy, DACiA

To obtain the wood anatomical features across transversal wood sections, we developed a new semi-automatic Matlab®-based software (DACiA), which is available upon request. Based on state-of-the-art thresholding techniques, the software automatically identifies the tracheid features of the radial rows initially marked along the tree rings, using segmented flexible lines. In short, Fourier analysis is used to decouple the image intensity profile into high- and low-frequency components. High frequencies are associated to the tracheid profile, whilst low frequencies correspond to variations in image acquisition and quality. The non-stationary signal is removed and the profile of the tracheid wall transitions is a stationary wave centred at zero. Then, tracheids are segmented using a constant zero threshold. Further on, a manual procedure corrects pixel by pixel possible measurement errors through an interactive graphic interface that helps to precisely delimitate tracheid lumens and walls. Finally, the software exports the measured anatomical features directly into their corresponding units of measurements to an Excel® or plain text file.

Climatic and environmental data

Monthly mean temperature and total precipitation values (period 1975–2006) were modelled at a spatial resolution of 180 m from discrete climatic data provided by the Spanish Meteorological Agency (<http://www.aemet.es>, accessed 18 Decembe 2013) (Ninyerola et al. 2007a,

2007b). Missing data for the 2007 and 2008 years were estimated by means of regression models using a second climatic dataset that was available from the Catalan Weather Service (<http://www.meteo.cat>, accessed 23 July 2013). Based on the available climatic data, the ratio between precipitation (P) and potential evapotranspiration (PET) was calculated (P/PET) and used as a drought index. The PET was estimated using the Hargreaves method (Hargreaves and Samani 1982).

Preliminary correlation analyses had shown that corresponding RW, EW and LW wood anatomical features responded to climatic variables averaged over different time periods. On the basis of these results and xylogenesis studies on Scots pine (Camarero et al. 1998, 2010), three different sets of P/PET measures, obtained from the meteorological data, were used in further analyses, covering the following time intervals: (1) from August (previous to growth year) to October of the year of tree-ring formation (named current year) for RW wood anatomical features (P/PET_{RW}); (2) from August (previous to growth year) to current June for EW wood anatomical features (P/PET_{EW}), and (3) from current May to current October for LW wood anatomical features (P/PET_{LW}).

Additionally, the standardized precipitation evapotranspiration index (SPEI) (Vicente-Serrano et al. 2010a, b) was used to explore the correlations between drought and the measured wood anatomical features at different time scales (1–12 months). The SPEI is a multi-scalar drought index that accounts for both the effects of temperature and precipitation on drought severity. The lower the SPEI value is, the drier the conditions are (Vicente-Serrano et al. 2010a, b). Based on previous analyses (Supplementary Fig. 2; Pasho et al. 2011), different SPEI time intervals were considered and used in further analyses to quantify time-dependent responses of wood anatomical features to drought stress (Supplementary Table 1).

Values of the CO₂ atmospheric concentration (C_a) were also used to account for their potential effects on the measured wood anatomical features. They were taken from the literature for the 1975–2003 period (Robertson et al. 2001; McCarroll and Loader 2004) and were estimated by means of linear regressions, based on the above-mentioned datasets, for the 2004–2008 period.

Statistical analyses

All variables were first checked for normality (Kolmogorov–Smirnov test) and logarithm transformed when necessary ($No.$ tracheids_{RW}, K_{hRW} , K_{hEW} , $(CWT/LD)_{EW}^2$, C_{costRW} , BAI). In the case of RD_{RW} (a count response variable) no transformation was applied, but a Poisson generalized mixed model was used (see below). The No.

Table 1 Statistical parameters of the wood anatomical features measured in living and dead trees

Variable (unit)	Statistics		Prades						Arcalís					
			RW		EW		LW		RW		EW		LW	
			Living trees	Dead trees	Living trees	Dead trees	Living trees	Dead trees	Living trees	Dead trees	Living trees	Dead trees	Living trees	Dead trees
No. tracheids	Mean		40	13	–	–	–	–	40	34	–	–	–	–
	SD		22.35	11.75	–	–	–	–	20.23	17.68	–	–	–	–
	CV		0.38	0.66	–	–	–	–	0.34	0.48	–	–	–	–
LD (μm)	Mean		20.81	16.87	26.85	21.97	–	–	19.82	19.25	26.26	25.52	–	–
	SD		3.31	3.34	3.70	3.87	–	–	3.08	2.70	3.53	3.58	–	–
	CV		0.14	0.17	0.13	0.16	–	–	0.13	0.13	0.11	0.12	–	–
CWT (μm)	Mean		11.16	9.29	–	–	11.73	8.91	10.28	10.73	–	–	11.21	12.38
	SD		1.40	1.48	–	–	2.17	1.83	1.68	1.50	–	–	2.55	2.28
	CV		0.12	0.14	–	–	0.16	0.18	0.14	0.14	–	–	0.17	0.15
K_h ($\text{kgMPa}^{-1}\text{s}^{-1}$)	Mean		3.E-06	5.E-07	3.E-06	5.E-07	–	–	2.E-06	2.E-06	2.E-06	2.E-06	–	–
	SD		2.E-06	6.E-07	2.E-06	6.E-07	–	–	2.E-06	1.E-06	2.E-06	1.E-06	–	–
	CV		0.68	0.96	0.68	0.95	–	–	0.59	0.64	0.59	0.63	–	–
$(\text{CWT/LD})^2$	Mean		–	–	0.27	0.27	–	–	–	–	0.20	0.24	–	–
	SD		–	–	0.13	0.13	–	–	–	–	0.08	0.13	–	–
	CV		–	–	0.41	0.42	–	–	–	–	0.34	0.40	–	–
C_{cost} (μm)	Mean		464	133	–	–	–	–	422	383	–	–	–	–
	SD		296	140	–	–	–	–	243	236	–	–	–	–
	CV		0.44	0.77	–	–	–	–	0.37	0.59	–	–	–	–
RD (no year^{-1})	Mean		1.75	0.85	–	–	–	–	1.67	1.38	–	–	–	–
	SD		1.23	1.00	–	–	–	–	1.18	1.13	–	–	–	–
	CV		0.72	1.09	–	–	–	–	0.69	0.84	–	–	–	–

Wood anatomical features were calculated for the whole ring (RW), for the earlywood (EW) or latewood (LW), respectively

LD radial lumen diameter, CWT cell wall thickness, K_h hydraulic conductivity, $(\text{CWT/LD})^2$ cell wall thickness to lumen diameter ratio raised to the second power, C_{cost} carbon cost investment,

RD number of resin ducts, CV coefficient of variation

tracheids_{RW} variable was not normalized to a standard number for all trees (Vaganov 1990), as raw data clearly showed large differences for this variable between living and dead trees.

Independent samples *t* tests were used to analyse differences in DBH and age between living and dead trees from Prades and Arcalís. Pearson and Spearman correlation coefficients (the Spearman coefficient was used only in the case of RD_{RW}) were used to quantify the associations between wood anatomical features and climatic variables (temperature, precipitation and SPEI), whilst linear regressions were conducted to assess temporal trends of annual climatic variables. To evaluate the time-related variability of each of the selected wood anatomical features, the coefficient of variation (CV) was calculated by dividing the standard deviation of each variable by its mean.

We used linear mixed-effects models to analyse the time trends of the wood anatomical features (No. tracheids_{RW}, LD_{EW}, CWT_{LW}, K_{hEW}, (CWT/LD)_{EW}² and C_{costRW}), the influence of the environmental variables (*C_a* and P/PET or SPEI) on them and the relationship between BAI and wood anatomical features (No. tracheids_{RW}, LD_{RW}, CWT_{RW}, K_{hRW} and C_{costRW}). A first set of models was fitted for each of the studied anatomical variables (No. tracheids_{RW}, LD_{EW}, CWT_{LW}, K_{hEW}, (CWT/LD)_{EW}² and C_{costRW}) to study their time trends. In each case, the fixed part of the model included the effects of tree condition (living vs. dead tree), site (Prades, Arcalís), the interaction condition × site, the covariate year (1975–2008), and the interactions condition × year, site × year, and condition × site × year.

A second set of models was fitted to analyse wood anatomy features (No. tracheids_{RW}, LD_{EW}, CWT_{LW}, K_{hEW}, (CWT/LD)_{EW}² and C_{costRW}) as a function of condition, site, the interaction condition × site, the covariate *C_a* and its interactions condition × *C_a*, site × *C_a*, and condition × site × *C_a*, and the covariate P/PET (or SPEI) and its interactions condition × P/PET (or SPEI), site × P/PET (or SPEI), and condition × site × P/PET (or SPEI).

Finally, a third set of models was fitted to study the response of BAI to different wood anatomical features (No. tracheids_{RW}, LD_{RW}, CWT_{RW}, K_{hRW} or C_{costRW}). In each case, the fixed part of the models included the effect of condition, site, the interaction condition × site, the corresponding wood anatomical feature and its interactions with condition, site, and condition × site.

In the case of the RD_{RW}, three Poisson generalized mixed models were fitted. The first model accounted for RD_{RW} time trends, and the second model evaluated the influence of the environmental variables (*C_a* and P/PET or SPEI) on RD_{RW}. These two models had the same structures as described above for the other selected wood anatomical

features. The third model accounted for the relationship between RD_{RW} and ring width, including the fixed effects of condition, site, the interaction condition × site, the covariate ring width, and the interactions condition × ring width, site × ring width, and condition × site × ring width.

In all mixed-effects models, tree identity was introduced as random effect and a first-order autoregressive covariance structure was used to account for temporal autocorrelation. To characterize differences between living and dead trees, the estimated marginal means were analysed, applying a Bonferroni correction to compare the main effects. If second-order interactions were significant, separate relationships for every site were considered. In all cases, coefficients were estimated using restricted maximum likelihood methods (REML), and relationships were considered significant at $P < 0.05$. Statistical analyses were carried out with SPSS (version 15.0, SPSS Inc., Chicago, IL) or R (version 3.0 packages, The R Foundation for Statistical Computing 2013).

Results

Patterns and trends of wood anatomical features in living and dead trees

The majority of wood anatomical features presented a significant negative time trend, the values of the dead trees being usually lower than those of the living trees, particularly at the more xeric Prades site (Fig. 1; Tables 1, 2). Overall, statistically significant differences ($P < 0.01$) were found between the living and dead trees for most anatomical features (No. tracheids_{RW}, LD_{EW}, K_{hEW}, C_{costRW} and RD_{RW}) (Fig. 1; Table 2). For all the aforementioned features, the predicted values (estimated marginal means) were always lower for the dead than for the living trees (results not shown). No statistically significant differences were found between living and dead trees in the case of the CWT_{LW} ($P = 0.086$) and (CWT/LD)_{EW}² features ($P = 0.454$). In Prades, the temporal variability (CV) of the wood anatomical features was always higher for the dead trees as compared to their living counterparts, whereas this was also observed in Arcalís except for LD_{RW}, CWT_{RW} and CWT_{LW} (Table 1).

The intercept and slope of the significant positive relationship between RD_{RW} and tree-ring width were similar for living and dead trees in Arcalís, whereas in Prades the intercept tended to be slightly higher for living trees and the slope was steeper for dead trees (Fig. 2; Supplementary Table 2).

Table 2 Results of linear mixed-effects models (estimates \pm SE) in which wood anatomical variables varied as a function of condition (living, dead), site (Prades, Arcalís) and year (from 1975 to 2008)

Variables	No. tracheids _{RW}	LD _{EW}	CWT _{LW}	K _{hEW}	(CWT/LD) _{EW} ²	C _{costRW}	RD _{RW}
Intercept	1.676 \pm 0.08 ^{***}	26.600 \pm 1.13 ^{***}	13.826 \pm 0.61 ^{***}	-5.727 \pm 0.13 ^{***}	-0.731 \pm 0.05 ^{***}	2.722 \pm 0.10 ^{***}	0.559 \pm 0.15 ^{***}
Living	0.099 \pm 0.11	-0.377 \pm 1.58	-1.999 \pm 0.86 [*]	0.052 \pm 0.18	0.005 \pm 0.01	0.071 \pm 0.13	0.321 \pm 0.20
Prades	-0.435 \pm 0.11 ^{**}	-2.387 \pm 1.59	-4.255 \pm 0.87 ^{***}	-0.480 \pm 0.19 [*]	0.082 \pm 0.07	-0.489 \pm 0.13 ^{**}	-0.531 \pm 0.22 [*]
Living \times Prades	0.418 \pm 0.16 [*]	2.420 \pm 2.24	4.923 \pm 1.22 ^{***}	0.658 \pm 0.26 [*]	0.108 \pm 0.10	0.520 \pm 0.19 [*]	0.521 \pm 0.29 ^{**}
Year	-0.014 \pm 0.00 ^{***}	-0.075 \pm 0.04 [*]	-0.101 \pm 0.02 ^{***}	-0.015 \pm 0.00 ^{***}	0.003 \pm 0.00	-0.016 \pm 0.00 ^{***}	-0.020 \pm 0.01 ^{**}
Living \times Year	0.000 \pm 0.00	0.083 \pm 0.05	0.066 \pm 0.03 [*]	0.004 \pm 0.01	-0.004 \pm 0.00	0.001 \pm 0.00	-0.005 \pm 0.01
Prades \times Year	-0.001 \pm 0.00	-0.083 \pm 0.05	0.056 \pm 0.03	-0.013 \pm 0.01 [*]	-0.000 \pm 0.00	-0.002 \pm 0.00	0.005 \pm 0.01
Living \times Prades \times Year	0.003 \pm 0.00	0.107 \pm 0.07	-0.066 \pm 0.04	0.012 \pm 0.01	-0.004 \pm 0.00	0.003 \pm 0.01	-0.001 \pm 0.01

Significant relationships at 0.05, 0.01 and 0.001 probability levels are marked with *, **, and ***, respectively. See Table 1 for the meaning of variables' abbreviations

Environmental influences on wood anatomical features

The overall response of the wood anatomical features to the P/PET was significant and positive, whereas C_a showed mainly negative relationships with those features but they were much lower in absolute terms (Table 3). The significant effects of P/PET did not depend on condition, site or the condition by site interaction for the majority of analysed features (No. tracheids_{RW}, CWT_{LW}, K_{hEW}, (CWT/LD)_{EW}² and C_{costRW}). In the case of the LD_{EW}, the significant effect of P/PET depended only on site (Table 3). In the case of CWT_{LW}, the significant relationship with C_a depended on the tree condition and its interaction with site (Table 3). For this anatomical feature, the two sites differed significantly between them ($P < 0.05$), with Prades presenting a significant positive difference between living and dead trees ($P < 0.01$) (results not shown). The association between C_a and K_{hEW} depended on site, but not on tree condition (Table 3).

The results of linear mixed-effects models were very similar if SPEI was used instead of P/PET to characterize climatic stress (Supplementary Table 3). Again, as in the case of P/PET most wood anatomical features were positively related to the SPEI drought index (Supplementary Table 3). In general, the strongest relationships between wood anatomical features and SPEI were observed from May to August, and dead trees tended to respond over longer time scales (by ca. 3 months) than living trees for most anatomical features (Supplementary Table 1; Supplementary Fig. 2). This means that dead trees showed a higher responsiveness to long-duration droughts in anatomical terms than living trees.

BAI association with wood anatomical features

BAI was significantly and positively related to several wood anatomical features (Supplementary Table 4), and this association was particularly strong with No. tracheids_{RW} (Fig. 3). For all the relationships of BAI with wood anatomical features, the estimated marginal means were always lower for the dead than for the living trees (results not shown), but this difference was significant only for LD_{RW} and CWT_{RW} ($P < 0.01$ in both cases).

Discussion

Surviving and now-dead Scots pine trees from Prades and Arcalís showed significant differences in their wood anatomical features in response to drought stress. Now-dead individuals usually presented smaller tracheids and a lower tracheid and resin duct production per growth ring than living trees, indicating that lower hydraulic capacity and

Table 3 Results of linear mixed-effects models (estimates \pm SE) in which wood anatomical variables varied as a function of condition (living, dead), site (Prades, Arcalís), C_a (atmospheric CO₂ concentrations) and P/PET (ratio between precipitation (P) and evapotranspiration (PET))

Variables	No. tracheids _{RW}	LD _{EW}	CWT _{LW}	K _{HEW}	(CWT/LD) _{EW} ²	C _{costRW}	RD _{RW}
Intercept	1.388 \pm 0.10 ^{***}	20.977 \pm 1.58 ^{***}	12.662 \pm 0.81 ^{***}	-6.111 \pm 0.21 ^{***}	-0.556 \pm 0.08 ^{***}	2.338 \pm 0.12 ^{***}	0.249 \pm 0.39
Living	-0.062 \pm 0.15	-0.056 \pm 2.22	-3.315 \pm 1.14 ^{**}	-0.043 \pm 0.29	0.007 \pm 0.11	-0.128 \pm 0.17	-0.291 \pm 0.53
Prades	-0.405 \pm 0.14 ^{**}	1.607 \pm 2.16	-3.985 \pm 1.13 ^{**}	-0.382 \pm 0.28	0.004 \pm 0.11	-0.379 \pm 0.17 [*]	-0.836 \pm 0.59
Living \times Prades	0.654 \pm 0.20 ^{**}	1.222 \pm 3.02	5.291 \pm 1.58 ^{**}	0.792 \pm 0.40 [*]	0.125 \pm 0.15	0.756 \pm 0.24 ^{**}	1.272 \pm 0.75
C_a	-0.008 \pm 0.00 ^{***}	-0.012 \pm 0.03	-0.059 \pm 0.01 ^{***}	-0.007 \pm 0.00 [*]	0.001 \pm 0.00	-0.008 \pm 0.00 ^{***}	-0.011 \pm 0.00 [*]
Living \times C_a	0.001 \pm 0.00	0.055 \pm 0.03	0.051 \pm 0.02 ^{**}	0.004 \pm 0.00	-0.002 \pm 0.00	0.002 \pm 0.00	0.001 \pm 0.01
Prades \times C_a	-0.002 \pm 0.00	-0.092 \pm 0.04 [*]	0.030 \pm 0.02	-0.011 \pm 0.00 [*]	0.001 \pm 0.00	-0.003 \pm 0.00	0.001 \pm 0.01
Living \times Prades \times C_a	0.001 \pm 0.003	0.072 \pm 0.05	-0.052 \pm 0.03 [*]	0.007 \pm 0.01	-0.003 \pm 0.00	0.000 \pm 0.00	-0.004 \pm 0.01
P/PET	0.436 \pm 0.10 ^{***}	7.154 \pm 1.42 ^{***}	2.071 \pm 0.96 [*]	0.488 \pm 0.21 [*]	-0.222 \pm 0.08 ^{**}	0.578 \pm 0.12 ^{***}	0.458 \pm 0.54
Living \times P/PET	0.241 \pm 0.14	-0.455 \pm 1.99	2.444 \pm 1.35	0.114 \pm 0.29	-0.000 \pm 0.11	0.296 \pm 0.17	0.885 \pm 0.71
Prades \times P/PET	0.057 \pm 0.15	-4.586 \pm 2.07 [*]	0.122 \pm 1.59	-0.039 \pm 0.30	0.069 \pm 0.12	-0.057 \pm 0.18	0.707 \pm 0.94
Living \times Prades \times P/PET	-0.372 \pm 0.21	1.871 \pm 2.88	-0.009 \pm 2.18	-0.169 \pm 0.42	-0.032 \pm 0.16	-0.358 \pm 0.25	-1.157 \pm 1.16

Significant relationships at 0.05, 0.01 and 0.001 probability levels are marked with *, ** and ***, respectively. See Table 1 for the meaning of variables' abbreviations

reduced investment of carbon into growth and defence characterized these mortality processes. Although our correlational approach precludes investigating the ultimate mechanisms of tree death, our results bring clear support to the idea that tree mortality is a complex process impacting the tree carbon and water economy (McDowell 2011; McDowell et al. 2011; Sevanto et al. 2014). The mechanisms underlying this process are not clear, but it is likely that the long-distance transport systems of the plant are involved (Anderegg et al. 2012) and could imply drought 'legacy' effects on the plant hydraulic system as recently reported for sudden aspen decline (Anderegg et al. 2013).

Both sites showed recent reductions in performance, as reflected in wood anatomical measurements (Fig. 1). This is consistent with the decline processes observed at the two sites and explains apparently counterintuitive results such as the negative relationship between CO₂ concentrations and xylem growth, which we interpret here as a response to warmer and drier conditions (Martínez-Vilalta et al. 2008). It should be also noted, however, that the two study sites showed important differences between them. In Prades, living and now-dead trees showed a long-term divergent hydraulic performance (chronic decline), whereas this divergence was less accentuated and more recent in Arcalís (acute decline).

High growth variability, for instance in terms of increased coefficient of variation of tree-ring width, has been associated to increased mortality risks (e.g., Ogle et al. 2000). Our results show that lower and more variable growth in now-dead compared to surviving individuals at the studied sites (Hereş et al. 2012) is associated to a higher variability in wood anatomical traits in now dead trees. This is consistent with Levanič et al. (2011), who also found a greater variability for the anatomical features of dying pedunculate oak (*Quercus robur* L.) trees in comparison with surviving individuals of the same species. Nevertheless, and in contrast to our findings, dying pedunculate oak trees studied by Levanič et al. (2011) presented wider conduits and higher specific hydraulic conductivity than surviving individuals until five years before death.

Our results show lower hydraulic conductivity in the stem xylem of now-dead trees, reflecting a lower water transport capacity over the whole studied period, particularly at the more xeric Prades site. This lower hydraulic capacity at the growth ring level does not necessarily translate into lower capacity to supply leaves with water, as concurrent changes in sapwood and leaf area need to be taken into account. However, the lower theoretical hydraulic conductivity in the earlywood of dead trees from Prades was observed throughout the study period and was greater in magnitude than the average defoliation levels currently observed in trees that are suffering drought-

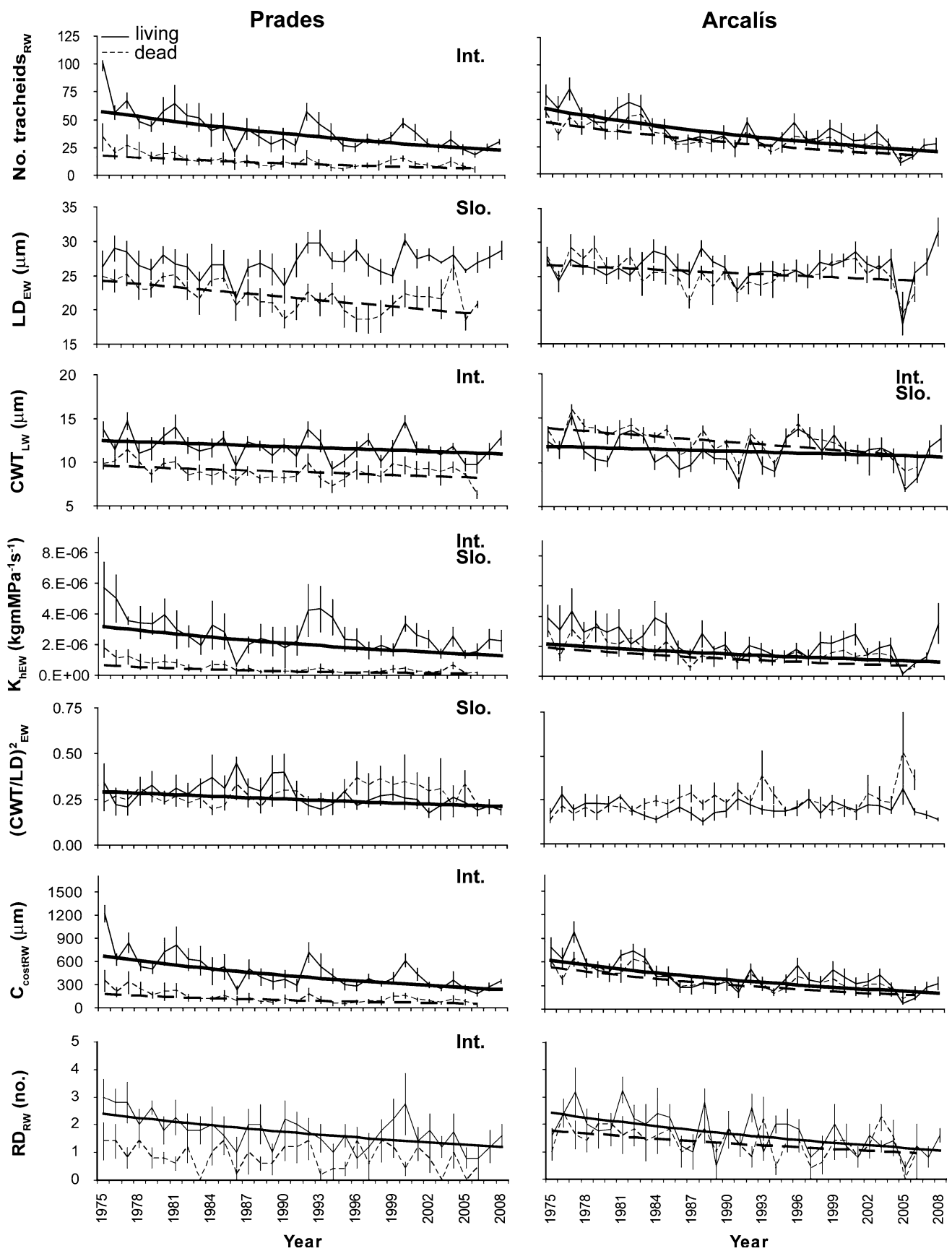


Fig. 1 Time trends of wood anatomical features (mean \pm SE) for living and dead trees in Prades and Arcalís study sites. Regression lines represent estimated slopes from the corresponding general (generalized in the case of RD_{RW}) linear mixed-effects models and they are represented only if significant. Significant differences between intercepts (*Int.*) and slopes (*Slo.*) of living and dead trees are indicated in the *top-right* corner of each panel, if present. Data for dead trees end in 2006, as this was the last year with a sample size higher than two trees. See Table 1 for the meaning of variables' abbreviations

induced mortality at this site (Poyatos et al. 2013). At the same time, the leaf-to-sapwood area ratio of defoliated and healthy trees at this site is similar (Poyatos, unpublished results), strongly suggesting that the measured reduction in hydraulic conductivity at the ring level was associated with lower capacity to support canopy water demands. Those findings observed in the drought-avoiding Scots pine contrast with those discussed before for the more drought-tolerant pedunculate oak (Levanič et al. 2011). Such apparently contradictory anatomical patterns between both species types may be linked to differences in their stomatal control of photosynthesis and the main physiological mechanism leading to drought-induced mortality. In pedunculate oak (relatively loose of stomatal control during drought), tree death is likely to be triggered by hydraulic failure, although carbon starvation or an interaction of both possible mechanisms of tree mortality cannot be discarded (Levanič et al. 2011). In Scots pine, instead, mortality seems to be primarily associated to the carbon economy and, in particular, with a long-term reduction in carbon uptake due to a combination of strict stomatal control, defoliation and reduced hydraulic capacity (Galiano et al. 2011; Poyatos et al. 2013; Aguadé et al. in review). The analysis of the response of wood anatomical features to SPEI showed that now-dead trees tended to respond to drought over longer time scales than surviving individuals. This result is consistent with a

general physiological slowdown previous to death and suggests a carryover effect on growth and hydraulic performance that constrains drought responses of trees prone to die (Anderegg et al. 2012).

We did not observe any difference between now-dead and surviving pines in the ratio between cell wall thickness and radial lumen diameter, here used as a proxy of vulnerability to xylem embolism (Hacke et al. 2001). This was due to the fact that in Prades tracheid lumens and cell wall thickness co-varied, and both variables presented lower values in now-dead individuals than in living trees (Fig. 1). This result is consistent with (1) previous reports showing limited plasticity of the vulnerability to embolism in Scots pine (Martínez-Vilalta and Piñol 2002; Martínez-Vilalta et al. 2009), and (2) our own measurements at the Prades site showing no difference in vulnerability to xylem embolism (in branches) between healthy and heavily defoliated pines (Poyatos et al. 2013). However, the applicability of the $(CWT/LD)^2$ index to the comparative analysis of healthy and declining individuals within a species might be problematic and we cannot completely rule out the possibility that this index may not be able to reflect true differences in vulnerability to embolism in this context.

Reduced hydraulic conductivity in now-dead trees resulted from the formation of narrow growth rings with narrow tracheids. At the same time, declining growth could be an indicator of low carbon availability. Under drought, whole-tree carbon assimilation tends to be impaired due to defoliation and stomatal closure (McDowell et al. 2008; Galiano et al. 2011). Although trees subjected to drought may allocate assimilates preferentially to other organs (e.g., buds, needles, roots) than to wood formation (Waring 1987; Eilmann et al. 2009), our own measurements at the Prades and Arcalís study sites indicate also lower reproductive investment in defoliated than healthy pines (Vilà-Cabrera et al. 2014). In our case, the low carbon investment

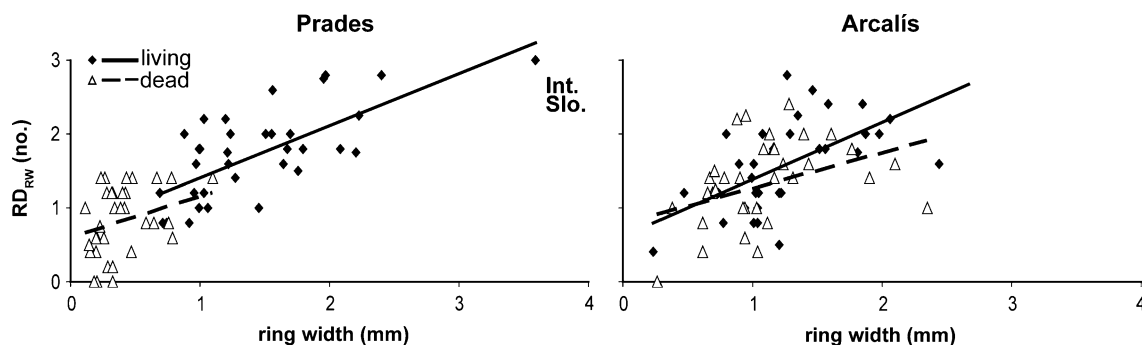


Fig. 2 Relationships between the number of resin ducts (RD_{RW}) and ring width for living and dead trees at the Prades and Arcalís sites. Regression lines represent slope estimates from the corresponding Poisson generalized mixed models and they are represented only if

significant. Significant differences between intercepts (*Int.*) and slopes (*Slo.*) of living and dead trees are indicated in the *top-right* corner of each panel, if present

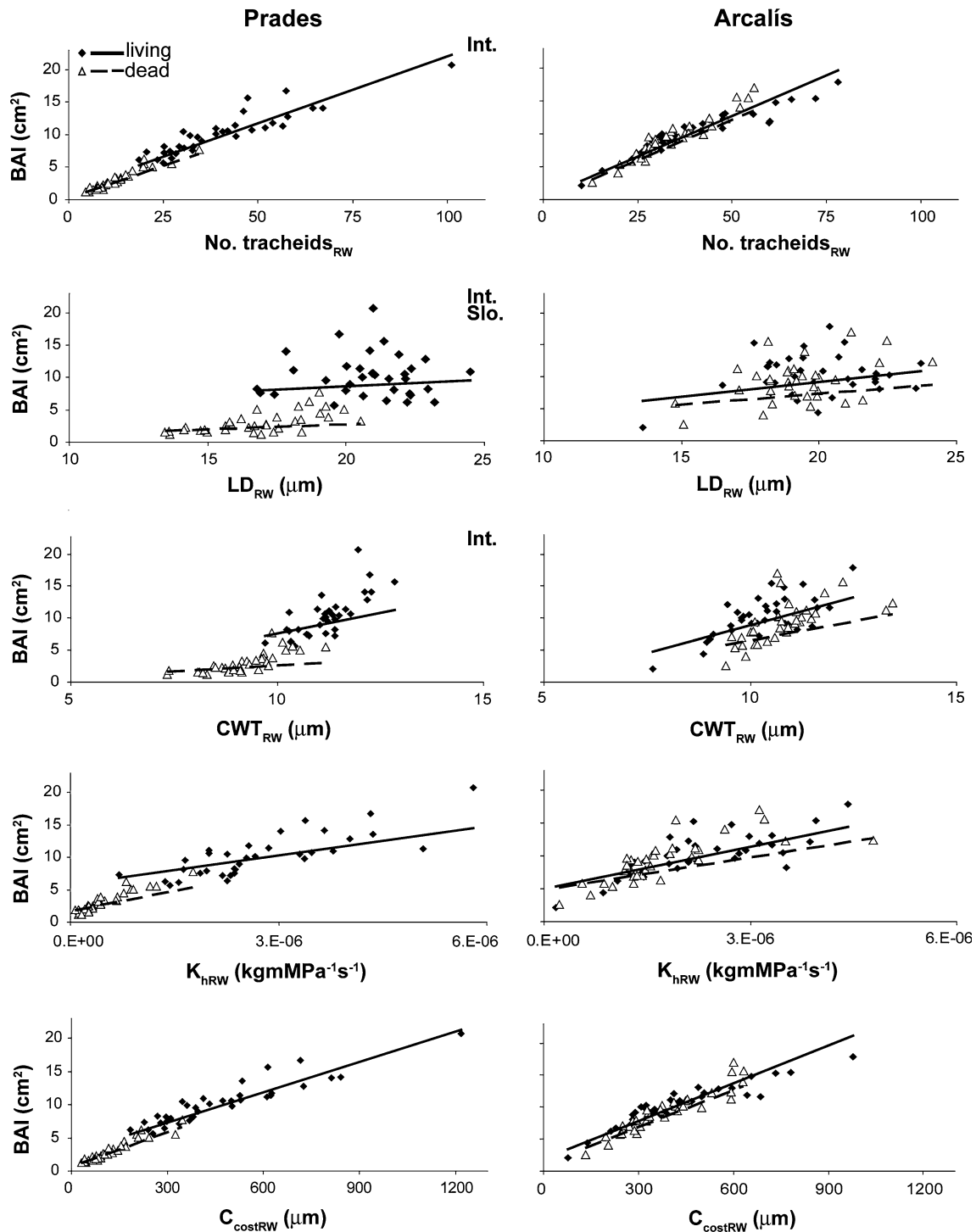


Fig. 3 Relationships between basal area increment (BAI) and wood anatomical features, measured for the whole ring, as indicated by the RW subscript. Regression lines represent slope estimates from the corresponding linear mixed-effects models and they are represented only if significant. Significant differences between intercepts (*Int.*)

and slopes (*Slo.*) of living and dead trees are indicated in the *top-right* corner of each panel, if present. See Table 1 for the meaning of variables' abbreviations

(in terms of C_{costRW} and RD_{RW}) was observed in the now-dead individuals from the more xeric Prades site. The lower production of resin ducts in now-dead trees is

consistent with previous results (Kane and Kolb 2010; Gaylord et al. 2013). Even though in our case bark beetles or other pests do not seem to be directly involved in the

mortality process (authors' personal observation), the reduced defence found in these chronically declining trees must be interpreted as an additional vulnerability factor. Depleted carbohydrate reserves have been reported in dying trees at both study sites (Galiano et al. 2011; Poyatos et al. 2013), suggesting that lower growth and resin duct production in dying trees might be associated to nearly exhausted or unavailable carbon reserves (Sala et al. 2012; Poyatos et al. 2013).

The growth reductions previously observed for the now-dead trees (Hereş et al. 2012) were more related to lower tracheid production than to a reduction in tracheid size (see also Camarero et al. 1998; Martin-Benito et al. 2013), thus minimizing the impact of reduced growth on hydraulic conductivity without increasing the carbon investment. Interestingly, cell wall thickness, a trait that is usually less variable than lumen size (Vaganov et al. 2006), showed high variability and a tighter positive relationship with BAI than lumen size. This result helps to explain why $(CWT/LD)_{EW}^2$ did not differ between living and now-dead trees, and it is again consistent with the notion that overall carbon availability may be constraining radial growth in the studied trees.

To conclude, we observed long-term changes in wood anatomical features predating tree death in Scots pine. We found different wood anatomical patterns between surviving and now-dead trees, with dead trees showing lower tracheid and resin duct production, and smaller lumen diameters than living trees. Those differences in wood anatomy were more pronounced in the more xeric (Prades) than in the more mesic (Arcalís) site, and they are consistent with the different forest decline dynamics observed at the two sites. At the xeric site, long-term growth reduction started on average 40 years before tree death, whereas at the mesic site, instead, growth started decreasing on average 15 years before tree death (Hereş et al. 2012). Carbohydrate depletion in the more xeric Prades site seems to be associated with long-term lowered hydraulic capacity in anatomical terms, whereas this pattern is not so clear in the mesic Arcalís site. In any case, the fact that the pace and pattern of the decline process differed substantially between the two study sites indicates that the wood anatomical responses and related mechanisms underlying drought-induced tree mortality vary amongst populations of the same species. This finding has implications for the monitoring and management of forests in drought-prone areas since early symptoms of decline, including changes in wood anatomy previous to tree death, differ markedly across sites.

Author contribution A.-M. Hereş participated in measuring wood samples, software development, statistical analyses and writing of the paper. J. J. Camarero

participated in statistical analyses, discussion and writing of the paper. B. C. López participated in the experimental design, software development and writing of the paper. J. Martínez-Vilalta participated in the experimental design, software development and writing of the paper.

Acknowledgments The authors thank H.A. Chaparro, A.Q. Alla, E. Pasho and M.C. Sancho for laboratory assistance. We also thank Debora Gil, who wrote all the Matlab codes for DACiA development. We are indebted to M. Mencuccini for field work and valuable discussions. The authors are also thankful to M. Ninyerola and the Catalan Meteorological Service for providing the two climatic datasets used in this study. Special thanks to M. Mejia-Chang for being part of our lives and a great inspiration for us all. This research was funded by the Spanish Ministry of Science and Innovation (projects CGL2007-60120, CSD2008-0040, CGL2010-16373, CGL2011-26654), a FPU PhD scholarship and a short stay at the IPE (CSIC).

Conflict of interest The authors declare that they have no conflict of interest.

References

- Allen CD, Macalady AK, Chenchouni H, Bachelet D, McDowell N, Vennetier M, Kitzberger T, Rigling A, Breshears DD et al (2010) A global overview of drought and heat-induced tree mortality reveals emerging climate change risks for forests. *For Ecol Manage* 259:660–684
- Anderegg WRL, Berry JA, Field CB (2012) Linking definitions, mechanisms, and modelling of drought-induced tree death. *Trends Plant Sci* 17:693–700
- Anderegg WRL, Plavcova L, Anderegg LDL, Hacke UG, Berry JA, Field CB (2013) Drought's legacy: multiyear hydraulic deterioration underlies widespread aspen forest die-off and portends increased future risk. *Global Ch Biol* 19:1188–1196
- Barbéro M, Loisel R, Quézel P, Richardson DM, Romane F (1998) Pines of the Mediterranean basin. In: Richardson DM (ed) *Ecology and biogeography of Pinus*. Cambridge University Press, Cambridge, pp 153–170
- Bigler C, Bräker OU, Bugmann H, Dobbervin M, Rigling A (2006) Drought as an inciting mortality factor in Scots pine stands of the Valais, Switzerland. *Ecosystems* 9:330–343
- Bréda N, Huc R, Granier A, Dreyer E (2006) Temperate forest trees and stands under severe drought: a review of ecophysiological responses, adaptation processes and long-term consequences. *Ann For Sci* 63:625–644
- Brodribb TJ, Cochard H (2009) Hydraulic failure defines the recovery and point of death in water-stressed conifers. *Plant Physiol* 149:575–584
- Camarero JJ, Guerrero-Campo J, Gutiérrez E (1998) Tree-ring growth and structure of *Pinus uncinata* and *Pinus sylvestris* in the Central Spanish Pyrenees. *Arct Alp Res* 30:1–10
- Camarero JJ, Olano JM, Parras A (2010) Plastic bimodal xylogenesis in conifers from continental Mediterranean climates. *New Phytol* 185:471–480
- Camarero JJ, Sangüesa Barreda G, Alla AQ, González de Andrés E, Maestro Martínez M, Vicente-Serrano SM (2012) Los precedentes y las respuestas de los árboles a sequías extremas revelan los procesos involucrados en el decaimiento de bosques mediterráneos de coníferas. *Ecosistemas* 21:22–30
- Catalan Bachiller G, Gil Muñoz P, Galera Peral RM, Martín Albertos S, Agundez Leal D, Alía Miranda R (1991) Las regiones de

- procedencia de *Pinus sylvestris* L. y *Pinus nigra* Arn. subsp. *salzmannii* (Dunal) Franco de España. INIA-ICONA, Madrid
- Cherubini P, Gartner BL, Tognetti R, Bräker OU, Schoch W, Innes JL (2003) Identification, measurement and interpretation of tree rings in woody species from Mediterranean climates. *Biol Rev* 78:119–148
- Choat B, Jansen S, Brodribb TJ, Cochard H, Delzon S, Bhaskar R, Bucci SJ et al (2012) Global convergence in the vulnerability of forests to drought. *Nature* 491:752–755
- Cochard H (1992) Vulnerability of several conifers to air embolism. *Tree Physiol* 11:73–83
- Cochard H, Froux F, Mayr S, Coutand C (2004) Xylem wall collapse in water-stressed pine needles. *Plant Physiol* 134:401–408
- Denne MP (1988) Definition of latewood according to Mork (1928). *IAWA Bull* 10:59–62
- Denne MP, Dodd RS (1981) The environmental control of xylem differentiation. In: Barnett JR (ed) *Xylem cell development*. Castle House, Kent, pp 236–255
- Eilmann B, Weber P, Rigling A, Eckstein D (2006) Growth reactions of *Pinus sylvestris* L. and *Quercus pubescens* Willd. to drought years at a xeric site in Valais Switzerland. *Dendrochronologia* 23:121–132
- Eilmann B, Zweifel R, Buchmann N, Fonti P, Rigling A (2009) Drought-induced adaptation of the xylem in Scots pine and pubescent oak. *Tree Physiol* 29:1011–1020
- Fonti P, von Arx G, García-González I, Eilmann B, Sass-Klaassen U, Gärtner H, Eckstein D (2010) Studying global change through investigation of the plastic responses of xylem anatomy in tree rings. *New Phytol* 185:42–53
- Fritts HC (2001) *Tree rings and climate*. Blackburn Press, New Jersey
- Galiano L, Martínez-Vilalta J, Lloret F (2010) Drought-induced multifactor decline of Scots pine in the Pyrenees and potential vegetation change by the expansion of co-occurring oak species. *Ecosystems* 13:978–991
- Galiano L, Martínez-Vilalta J, Lloret F (2011) Carbon reserves and canopy defoliation determine the recovery of Scots pine 4 yr after a drought episode. *New Phytol* 190:750–759
- Gaylord ML, Kolb TE, Pockman WT, Plaut JA, Yezzer EA, Macalady AK, Pangle RE, McDowell NG (2013) Drought predisposes piñon-juniper woodlands to insect attack and mortality. *New Phytol* 198:567–578
- Giorgi F, Lionello P (2008) Climate change projections for the Mediterranean region. *Glob Planet Ch* 63:90–104
- Hacke UG, Sperry JS, Pockman WT, Davis SD, McCulloh KA (2001) Trends in wood density and structure are linked to prevention of xylem implosion by negative pressure. *Oecologia* 126:457–461
- Hargreaves GH, Samani ZA (1982) Estimating potential evapotranspiration. *J Irrig Drain Div ASCE* 108:225–230
- Hereş AM, Martínez-Vilalta J, Claramunt López B (2012) Growth patterns in relation to drought-induced mortality at two Scots pine (*Pinus sylvestris* L.) sites in NE Iberian Peninsula. *Trees Str Funct* 26:621–630
- Hereter A, Sánchez JR (1999) Experimental areas of Prades and Montseny. In: Bellot J, Rodà F, Retana J, Gracia CA (eds) *Ecology of Mediterranean evergreen Oak forests*. Springer, Germany, pp 15–27
- Hsiao TC, Acevedo E (1974) Plant responses to water deficits, water-use efficiency, and drought resistance. *Agric Meteorol* 14:59–84
- IPCC (2013) *Climate Change 2013: the Physical Science Basis*. Contribution of Working Group I to the Fifth Assessment Report of the Intergovernmental Panel on Climate Change. Cambridge University Press, Cambridge
- Irvine J, Perks MP, Magnani F, Grace J (1998) The response of *Pinus sylvestris* to drought: stomatal control of transpiration and hydraulic conductance. *Tree Physiol* 18:393–402
- Kane JM, Kolb TE (2010) Importance of resin ducts in reducing ponderosa pine mortality from bark beetle attack. *Oecologia* 164:601–609
- Köppen W (1936) Das Geographische System der Klimate. In: Köppen W, Geiger R (eds) *Handbuch der Klimatologie*. Gebrüder Borntraeger, Berlin, pp 1–44
- Levanič T, Čater M, McDowell NG (2011) Associations between growth, wood anatomy, carbon isotope discrimination and mortality in a *Quercus robur* forest. *Tree Physiol* 31:298–308
- Martin-Benito D, Beeckman H, Cañellas I (2013) Influence of drought on tree rings and tracheid features of *Pinus nigra* and *Pinus sylvestris* in a mesic Mediterranean forest. *Eur J For Res* 132:33–45
- Martínez-Vilalta J, Piñol J (2002) Drought-induced mortality and hydraulic architecture in pine populations of the NE Iberian Peninsula. *For Ecol Manage* 161:247–256
- Martínez-Vilalta J, López BC, Adell N, Badiella L, Ninyerola M (2008) Twentieth century increase of Scots pine radial growth in NE Spain shows strong climate interactions. *Glob Ch Biol* 14:1–14
- Martínez-Vilalta J, Cochard H, Mencuccini M, Sterck F, Herrero A, Korhonen JFJ, Llorens P, Nikinmaa E, Nollé A, Poyatos R, Ripullone F, Sass-Klaassen U, Zweifel R (2009) Hydraulic adjustments of Scots pine across Europe. *New Phytol* 184:353–364
- Martínez-Vilalta J, Aguadé D, Banqué M, Barba J, Curiel Yuste J, Galiano L, García N, Gómez M, Hereş AM, López BC, Lloret F, Poyatos R, Retana J, Sus O, Vayreda J, Vilà-Cabrera A (2012) Las poblaciones ibéricas de pino albar ante el cambio climático: con la muerte en los talones. *Ecosistemas* 21:15–21
- Martín JA, Esteban LG, de Palacios P, García Fernández F (2010) Variation in wood anatomical traits of *Pinus sylvestris* L. between Spanish regions of provenance. *Trees Str Funct* 24:1017–1028
- Matías L, Jump AS (2012) Interactions between growth, demography and biotic interactions in determining species range limits in a warming world: the case of *Pinus sylvestris*. *For Ecol Manage* 282:10–22
- Matlab (2010) Mathworks Company, Version 7.10 R2010a. Natick, Massachusetts
- McCarroll D, Loader NJ (2004) Stable isotopes in tree rings. *Quat Sci Rev* 23:771–801
- McDowell NG (2011) Mechanisms linking drought, hydraulics, carbon metabolism, and vegetation mortality. *Plant Physiol* 155:1051–1059
- McDowell NG, Sevanto S (2010) The mechanisms of carbon starvation: how, when, or does it even occur at all? *New Phytol* 186:264–266
- McDowell N, Pockman WT, Allen CD, Breshears DD, Cobb N, Kolb T, Plaut J, Sperry J, West A, Williams DG, Yezzer EA (2008) Mechanisms of plant survival and mortality during drought: why do some plants survive while others succumb to drought? *New Phytol* 178:719–739
- McDowell NG, Beerling DJ, Breshears DD, Fisher RA, Raffa KF, Stitt M (2011) The interdependence of mechanisms underlying climate-driven vegetation mortality. *Trends Ecol Evol* 26:523–532
- Nikolov N, Helmisaari H (1992) Silvics of the circumpolar boreal forest tree species. In: Shugart H, Leemans R, Bowan G (eds) *A systems analysis of the global boreal forest*. Cambridge University Press, Cambridge, pp 13–84
- Ninyerola M, Pons X, Roure JM (2000) A methodological approach of climatological modeling of air temperature and precipitation through GIS techniques. *Int J Climatol* 20:1823–1841
- Ninyerola M, Pons X, Roure JM (2007a) Monthly precipitation mapping of the Iberian Peninsula using spatial interpolation tools

- implemented in a geographic information system. *Theor Appl Climatol* 89:195–209
- Ninyerola M, Pons X, Roure JM (2007b) Objective air temperature mapping for the Iberian Peninsula using spatial interpolation and GIS. *Int J Climatol* 27:1231–1242
- Ogle K, Whitham TG, Cobb NS (2000) Tree-ring variation in pinyon predicts likelihood of death following severe drought. *Ecology* 81:3237–3243
- Paine TD, Raffa KF, Harrington TC (1997) Interactions among scolytid bark beetles, their association fungi, and live host conifers. *Ann Rev Entomol* 42:179–206
- Pasho E, Camarero JJ, de Luis M, Vicente-Serrano SM (2011) Impacts of drought at different time scales on forest growth across a wide climatic gradient in north-eastern Spain. *Agric For Meteorol* 151:1800–1811
- Piñol J, Terradas J, Lloret F (1998) Climate warming, wildfire hazard, and wildfire occurrence in coastal Eastern Spain. *Clim Ch* 38:345–357
- Pons X (1996) Estimación de la radiación solar a partir de modelos digitales de elevaciones. Propuesta metodológica. In: Juaristi J, Moro I (eds) VII Coloquio de Geografía Cuantitativa. Sistemas de Información Geográfica y Teledetección, Vitoria-Gasteiz, Spain, pp 87–97
- Poyatos R, Aguadé D, Galiano L, Mencuccini M, Martínez-Vilalta J (2013) Drought-induced defoliation and long periods of near-zero gas exchange play a key role in accentuating metabolic decline of Scots pine. *New Phytol* 200:388–401
- R (2013) R: A language and environment for statistical computing, Version 3.0. R foundation for statistical computing, Vienna, Austria
- Rigling A, Brühlhart H, Bräker OU, Forster T, Schweingruber FH (2003) Effects of irrigation on diameter growth and vertical resin duct production in *Pinus sylvestris* L. on dry sites in the central Alps Switzerland. *For Ecol Manage* 175:285–296
- Rigling A, Bigler C, Eilmann B, Feldmeyer-Christe E, Gimmi U, Ginzler C, Graf U, Mayer P, Vacchiano G, Weber P, Wohlgenuth T, Zweifel R, Dobbertin M (2013) Driving factors of a vegetation shift from Scots pine to pubescent oak in dry Alpine forests. *Glob Ch Biol* 19:229–240
- Robertson A, Overpeck J, Rind D, Mosley-Thompson E, Zielinski G, Lean J, Koch D, Penner J, Tegen I, Healy R (2001) Hypothesized climate forcing time series for the last 500 years. *J Geophys Res* 106:14783–14803
- Sala A, Piper F, Hoch G (2010) Physiological mechanisms of drought-induced tree mortality are far from being resolved. *New Phytol* 186:274–281
- Sala A, Woodruff DR, Meinzer FC (2012) Carbon dynamics in trees: feast or famine? *Tree Physiol* 32:764–775
- Seo J-W, Smiljanić M, Wilmking M (2014) Optimizing cell-anatomical chronologies of Scots pine by stepwise increasing the number of radial tracheid rows included—Case study based on three Scandinavian sites. *Dendrochronologia* 32:205–209
- Sevanto S, McDowell NG, Dickman LT, Pangle R, Pockman WT (2014) How do trees die? A test of the hydraulic failure and carbon starvation hypotheses. *Plant, Cell Environ* 37:153–161
- SPSS (2006) IBM Company, Version 15.0. Chicago, Illinois
- Tyree MT, Zimmerman MH (2002) Xylem structure and the ascent of sap. Springer, New York
- Vaganov EA (1990) The tracheidogram method in tree-ring analysis and its application. In: Cook ER, Kairiukstis LA (eds) Methods of dendrochronology: applications in the environmental sciences. Kluwer Academic Publishers, Dordrecht, pp 63–76
- Vaganov EA, Hughes MK, Shashkin AV (2006) Growth dynamics of conifer tree rings: images of past and future environments. Springer, New York
- Vicente-Serrano SM, Beguería S, López-Moreno JJ (2010a) A multi-scalar drought index sensitive to global warming: the standardized precipitation evapotranspiration index. *J Clim* 23: 1696–1718
- Vicente-Serrano SM, Beguería S, López-Moreno JJ, Angulo M, El Kenawy A (2010b) A new global 0.5° gridded dataset (1901–2006) of a multiscale drought index: comparison with current drought index datasets based on the Palmer drought severity index. *J Hydrometeorol* 11:1033–1043
- Vilà-Cabrera A, Martínez-Vilalta J, Galiano L, Retana J (2013) Patterns of forest decline and regeneration across Scots pine populations. *Ecosystems* 16:323–335
- Vilà-Cabrera A, Martínez-Vilalta J, Retana J (2014) Variation in reproduction and growth in declining Scots pine populations. *Persp Plant Ecol Evol Syst* 16:111–120
- von Wilpert K (1991) Intraannual variation of radial tracheid diameters as monitor of site specific water stress. *Dendrochronologia* 9:95–113
- Vysotskaya LG, Vaganov EA (1989) Components of the variability of radial cell size in tree rings of conifers. *IAWA Bull* 10:417–428
- Waring RH (1987) Characteristics of trees predisposed to die. *Bioscience* 37:569–574
- Wimmer R (2002) Wood anatomical features in tree-rings as indicators of environmental change. *Dendrochronologia* 20:21–36
- Zweifel R, Zimmermann L, Zeugin F, Newbery DM (2006) Intra-annual radial growth and water relations of trees: implications towards a growth mechanism. *J Exp Bot* 57:1445–1459